Applications of Microelectrodes to Problems in Chemical Oceanography

Clare E. Reimers

College of Oceanic and Atmospheric Sciences, Oregon State University, Hatfield Marine Science Center, Newport, Oregon 97365

Received August 9, 2006

Contents

Clare E. Reimers is a professor in the College of Oceanic and Atmospheric Sciences of Oregon State University and her laboratory is located within OSU's Hatfield Marine Science Center (Newport, OR). Her areas of specialization are benthic biogeochemistry and applied electrochemistry with emphasis on in situ measurements of redox conditions in natural waters and sediments and the marine carbon cycle. She currently serves the chemical oceanographic community as a member of the Ocean Research Interactive Observatory Networks (ORION) Observatory Steering Committee, The University National Ocean Laboratories (UNOLS) Fleet Improvement Committee and as an associate editor for *Limnology and Oceanography: Methods.*

1. Introduction

Many of the remarkable biogeochemical processes that regulate the transfer of mass and energy between the atmosphere, ocean waters, benthos, and earth's crust take place at small spatial scales, e.g., within single cells, pores of sediments and rocks, aggregates, microbial mats, or biofilms. Over the past two decades, with advances in electroanalytical chemistry and microelectronics technology it has become progressively possible to probe marine microenvironments and interfaces and discover how marine chemistry and life interact. Some of this exploration has been in the laboratory, but a significant portion has been possible because of in situ techniques designed for extreme or dynamic environments (e.g., euxinic seas, the deep seafloor, hydrothermal vents). This paper reviews the role that microelectrodes have played (prior to the calendar year 2007) in providing fundamental information about the chemical reactions which structure the marine environment. The intent is to illustrate inventive applications that have contributed new insight about oceanic processes and chemical speciation rather than to critique different sensor designs, operating characteristics, or methodologies. However, where appropriate, original and review articles that emphasize fundamental sensing principles or the promise of new materials or integrated analytical systems will be cited to also give the reader a view of current developmental work on chemical sensors.

2. Defining Microelectrodes

The term "microelectrode" is used to refer to both electrochemical sensors and very small electroactive surfaces embodied within sensors or larger analytical systems (Figure 1).[1] Those that are the focus of this review are constructed with single (rather than array) electrode surfaces confined within or just behind the tip of a cylindrical glass or PEEK (polyethyl ether ketone) capillary, so that the electroactive surface area determines many of their temporal and spatial response characteristics (Table 1). Each variety of microelectrode will return an electrical signal (e.g., a current or potential) in response to a particular chemical species or be able to detect and resolve a number of different species at the same time.[2] In many texts, the definition of microelectrodes is limited to electrodes with diameters of tens of micrometers or less, and this distinction is usually because at this scale, even in a turbulent flow regime, the flux of an analyte to the electrode surface will be controlled by radial diffusion.[3] This condition has the advantage that a steady-state faradaic response is attained very rapidly and nearly independent of stirring or natural convection for amperometric and voltammetric microsensors. However, because relatively large electrodes ($0.03 \leq 2r \leq 1$ mm; sometimes called "minielectrodes") may, under nonturbulent conditions such as those found in the interstitial spaces of fine-grained sediments, respond like a microelectrode,[4] certain electrochemical sensors with these electrode dimensions and tailored techniques will be included in this review.

10.1021/cr050363n CCC: $65.00
Published on Web 01/26/2007

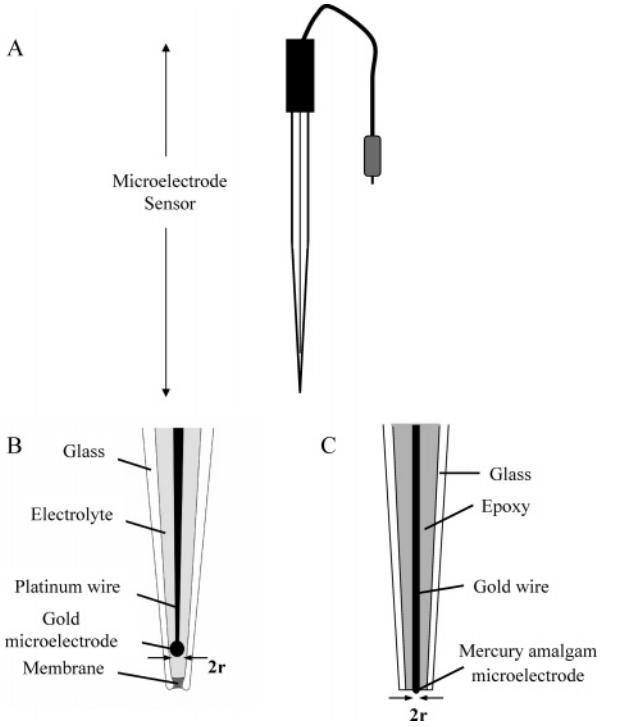

Figure 1. Schematic drawings illustrating the double usage of the term "microelectrode" as both an electrochemical sensor (A) and a tiny sensing surface, often located in the tip region of glass capillary constructions (B and C). B resembles the tip of a Clark-type O_2 microelectrode and C the tip of a Au-amalgam voltammetric microelectrode. Microelectrode applications require equipment for measuring electrical quantities in a complete electrochemical cell, but these components are considered part of a larger analytical system rather than part of the sensor.

3. Types of Microelectrodes in Chemical Oceanography

There are more than a dozen aquatic chemical species or parameters that may be measured with microelectrodes, and several earlier reviews present detailed information about the great variety of microsensor designs that have been developed and their detection principles, construction, measuring equipment, interferences, application methods, and experimental concerns.[5−10] Among the many designs, the three single microelectrode sensors that have been most widely used in situ and in laboratory investigations of marine samples are the amperometric "Clark-type" oxygen microelectrode, the potentiometric glass pH microelectrode, and the voltammetric mercury-plated microelectrode (with images of representative examples given in Figure 2). Each of these sensors is presently commercially available and can be fabricated with a range of tip sizes and corresponding performance specifications (Table 2). Their extensive use is because spatial and temporal variations in dissolved oxygen, pH, and several sulfur and trace metal species measurable by voltammetry are ultimately linked to the ocean's most ubiquitous and important chemical reactions. Below a brief overview of these sensors will be followed by looking at their most significant oceanographic applications.

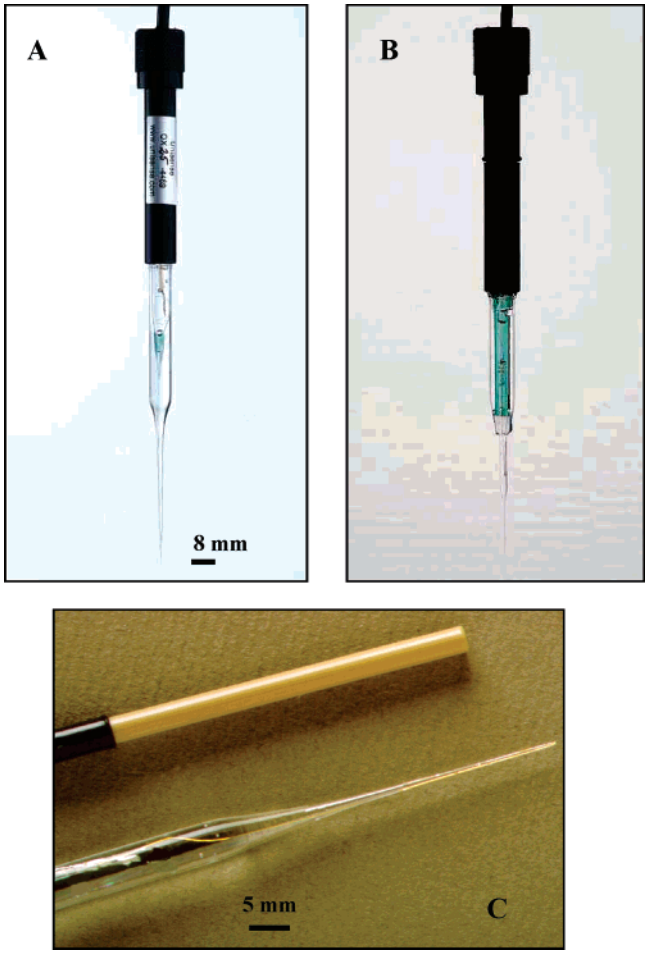

Figure 2. (A) Clark-type oxygen microelectrode (courtesy Unisense A/S, Aarhus DK); (B) glass pH microelectrode (Unisense A/S); (C) voltammetric electrodes constructed in PEEK and glass capillaries (courtesy of G. W. Luther III).

3.1. Clark-type Oxygen Microelectrode

The Clark-type oxygen microelectrode senses dissolved oxygen after its diffusion across a silicone membrane enclosed at the tip.[11] Technically, the sensor is not one electrode but three for it incorporates a complete electrochemical cell and a guard cathode whose purpose is to strip oxygen from the backing electrolyte solution. It is operated using the technique of chronoamperometry, giving rise to a cathodic current typically measured in picoamperes (pA). Its use in the aquatic sciences was preceded by measurements with an uncombined Au-plated Pt microelectrode with a recessed tip and resin coating.[12,13]

A model equation for predicting the signal of Clark-type O_2 microelectrodes from the physical dimensions of the tip, O_2 partial pressure, and diffusion properties of the electrolyte and membrane was presented and validated experimentally

Table 1. Definitions of Spatial and Temporal Response Characteristics of Microelectrodes

characteristic	definition
spatial resolution	measure of the size of the area of the environment that contributes to the sensor signal
response time	time required for a sensor signal to reach a percentage (usually 90%) of the total signal change after an abrupt change in analyte concentration
stirring effect or sensitivity	percent change in sensor signal when transitioning from a stagnant to a vigorously agitated fluid
signal sensitivity	relative change in sensor signal for a change in analyte concentration; often equated to the slope of a linear calibration

Table 2. Characteristics of the Three Types of Single Microelectrode Sensors That Have Been Widely Applied in Chemical Oceanography

	Clark-type O_2 amperometric	glass pH potentiometric	Hg-plated voltammetric
tip outer diameter	5−1000[a] μm	10−1000 μm	50−3175[a] μm
electrode[b] diameter	1−10 μm	10−1000 μm	5−100 μm
sensor type	combined gas microsensor with ion-impermeable membrane	uncombined ion-exchange-based glass membrane sensor, used with a separate reference electrode	uncombined bare or agarose gel-integrated working electrode, used with separate reference and counter electrodes
90% response time	0.2−4 s	<60 s	seconds−minutes and dependent on the voltammetric technique
signal sensitivity at 20 °C	0.2−1 pA/μM O_2 (see Figures 3 and 4)	58.1 mV/pH unit	0.02−30 nA/μM and dependent on the electrode diameter, chemical species, and voltammetric technique applied
references	11, 19, 91	5, 25−29	10, 30−33, 40[c]

[a] For some applications where spatial resolution is not critical, sensors have been made with a thick tip to be rugged. For the Clark-type O_2 sensor this is done by thickening the glass capillary wall around a membrane-filled opening of only a few micrometers. The pipettes of voltammetric electrodes have been made intentionally wide and filled with nonconductive epoxy. [b] In this context, "electrode" refers to the electroactive surface that may be exposed at the tip or enclosed behind a membrane as in Figure 1B and C. [c] Xu, K.; Dexter, S. C.; Luther, G. W., III. *Corrosion* **1998**, *54*, 814.

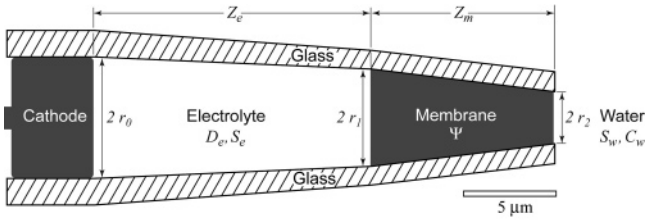

Model equation for the O_2 reduction current

$$I = \Phi \pi r_1 p_{O_2} \left(\frac{Z_m}{r_2 \Psi} + \frac{Z_e}{r_0 D_e S_e} \right)^{-1}$$

Figure 3. Schematic drawing of the very tip of a Clark-type O_2 microelectrode, and model equation for predicting the O_2 reduction current (output signal − zero current, A) as a function of p_{O2} = partial pressure of O_2 (Pa), Z_m and Z_e = thicknesses (m) of silicone membrane and electrolyte, Ψ = O_2 permeability of the silicone membrane (mol m^{-1} Pa^{-1} s^{-1}), D_e = O_2 diffusion coefficient in the electrolyte (m^2 s^{-1}), S_e = O_2 solubility in the electrolyte (mol m^{-3} Pa^{-1}), and r_o, r_1, and r_2 = the internal sensor radii (m) at the cathode and inner and outer boundaries of the membrane. A conversion factor Φ = coulombs per mole O_2 reduced. Modified with permission from ref 14. Copyright 1998 by the American Society of Limnology and Oceanography, Inc.

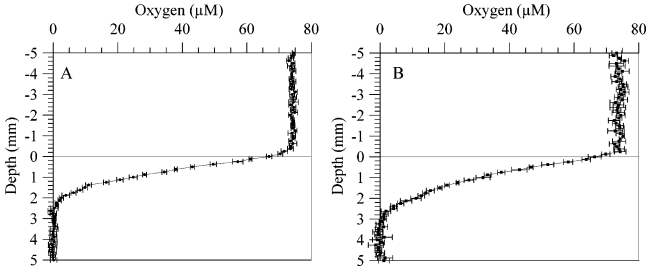

Figure 4. Two oxygen profiles measured in situ and simultaneously at the sea floor on the Oregon margin (110 m water depth) with Clark-type microelectrodes having tip outer diameters of 25 μm (Unisense OX-25 sensors). Each sample point represents the mean and standard deviation of five readings taken with a 1 s delay between readings. The higher average signal-to-noise ratio of sensor A compared to sensor B produced a profile in which the oxygen zero depth is resolved with greater certainty. However, the diffusive oxygen utilization rate when predicted from the DBL gradient of A is 25% lower than the same rate predicted from modeling the curvature of the whole profile (0.34 versus 0.45 μmol cm^{-2} day^{-1}). The corresponding rate derived for profile B is 0.34 μmol cm^{-2} day^{-1} by either method. These data were collected by the author in 2004.

by Gundersen et al.[14] (Figure 3). This model and similar formulations for the signals of macromembrane-covered oxygen electrodes[15,16] stem from the principles used to derive the Cottrell equation,[17] which also predicts a time-dependent concentration profile at an electrode surface after application of a constant potential.[18] Ideally, Clark-type oxygen microelectrodes restrict the diffusive concentration gradient of dissolved oxygen to within the sensor. When this condition is met, as is assumed for the model in Figure 3, the sensor is insensitive to stirring. For sensors where $r_o \approx r_1 \approx r_2$, increasing the ratio of $r_2/(Z_m + Z_e)$ can extend the oxygen gradient to outside the sensor, causing a stirring effect.[14] However, a relatively greater r_o will increase the sensor signal sensitivity, while decreasing ($Z_m + Z_e$) will shorten the response time. Thus, there is a tradeoff between sensor response characteristics with a middle ground preferred by most users. Other small adjustments that can improve the signal of a Clark-type O_2 microelectrode at a given P_{O2} and temperature (without sacrificing stirring independence) are a greater relative membrane thickness ($Z_m/[Z_e + Z_m]$) and a more conical-shaped tip ($r_o > r_2$).[14,19] Without an adequate signal-to-noise ratio, it can be difficult to precisely resolve oxygen microgradients or the onset of anoxic conditions in the marine environment. Microelectrode performance in situ may also differ from predeployment evaluations due to pressure influences on the sensor or changes in noise sources and recording. Two oxygen profiles measured simultaneously at the sea floor but with Clark-type microelectrodes with differing signal-to-noise ratios are illustrated in Figure 4. In this example, the higher noise and lower signal sensitivity (0.45 pA/μM) of sensor B compared to A (0.59 pA/μM) makes the second profile less precise.

3.2. Glass pH Microelectrodes

The glass pH microelectrode is an example of a miniaturized ion-selective electrode that senses the activity of H^+ because of a membrane potential created as a consequence of selective charge exchange between the outer solution and the hydrated pH glass.[20] The protruding pH glass tip may be fabricated into a sharp point or bulb, and recessed tips are also workable.[21] The persistence of glass pH microelectrodes (and minielectrodes) in oceanographic research is an indication that they are more rugged, have better longevity, and are more available than many newer varieties of pH microsensors including polymeric liquid membrane pH microelectrodes,[22] sol−gel-based optodes,[23] and solid-state electrodes.[25] One adaptive application of the pH microelectrode has been its incorporation into a pCO_2 sensor.[27]

The potentiometric measurement of pH requires a high impedance voltmeter and a nearby reference electrode such as a silver−silver chloride electrode (SSCE) to complete the electrochemical cell.[28] Response times are typically less than

a minute (Table 2) but dependent on the pH glass thickness and the magnitude of the pH shift.[29] One of the greatest challenges for field applications of pH microelectrodes is eliminating sources of drift. Drift in the sensor signal under constant temperature and pressure conditions may be caused by adhesion of natural materials to the pH glass, changes in the liquid junction potential of the reference, or leakage currents through the reference. These factors have limited the precision of pH microelectrode measurements to at best ±0.01 pH units during marine applications.

3.3. Voltammetric Sensors

Robust mercury-plated microelectrodes with hemispherical geometry that are used with voltammetric techniques such as cyclic voltammetry and square-wave anodic stripping voltammetry (SWASV) were introduced to the aquatic sciences by Tercier et al.[30] and Brendel and Luther.[31] Their development for in situ measurements has progressed in two directions: (1) fabrication on an electro-etched Ir substrate (polished electrode $2r = 5-16\ \mu$m) in combination with an agarose gel antifouling membrane[32] and (2) fabrication on a Au wire substrate (usually $2r = 100\ \mu$m) without a membrane (Figure 1c).[33] The intended field applications of the two designs impose radically different operational and performance requirements. The first enables highly sensitive measurements of dissolved trace metals such as Cd and Pb without interferences from colloidal and/or macromolecular materials and was developed primarily for water column studies. The gel layer is usually 0.3−1 mm thick and ensures purely diffusive transport of ions to the microelectrode surface. Sensitivity is dependent on deposition times that are typically 5−15 min in duration before applying SWASV conditions.[34] The most recent advancements have been interconnected and individually addressable gel integrated Ir-based microelectrode (GIME) arrays[35,36] and their modification to include a metal-complexing resin (CGIME).[10] By incorporating both varieties of sensor into a Multi Physical Chemical Profiler equipped with three separate microflow through systems (a flow-injection analysis system for on-line sample pretreatment, controlling hardware, and software), free ion and dynamic fractions of trace metals have been monitored in coastal waters down to subnanomolar levels together with total extractable metal concentrations.[37] Recent reviews of these developments stress the significance that these microelectrodes are able to detect chemical species based on their chemical reactivity and mobility.[10,38] This capability means that they have great potential for monitoring bioavailable and other environmentally relevant groups of trace metal species.[10]

The second variety of voltammetric sensor, the Au-amalgam electrode, was developed primarily for the concurrent measurement of O_2, Mn^{2+}, Fe^{2+}, I^-, and /or forms of reduced S at micromolar concentrations in the pore waters of marine and freshwater sediments[39] with subsequent work on other complex natural samples enriched with either these or additional Mn, Fe, Pb, and /or S species (see section 4.4).[40] Their larger size and bare mercury layer can withstand the physical abrasion of sediments but limits their ability to produce voltammograms that can be interpreted quantitatively when exposed to turbulent flow.[41] However, some of these effects have been overcome by using rapid scan rates (≥1000 mV s^{-1} with either cyclic or linear sweep voltammetry) and by enclosing the voltammetric electrode (and reference and counter electrodes) in flow-through cells or "wands" that can control or restrict flow across the electrode.[42] Examples of such applications are discussed below. The greatest remaining challenges associated with voltammetric microelectrode measurements are refinement of techniques to optimize sensitivity, simplify calibration, and eliminate complicated interactions that occur when multiple reactive species are oxidized or reduced at the electrode surface. In other words, this kind of work relies on paying careful attention to the details of voltammetric techniques that can produce species at a mercury surface that are not present in situ. This means these sensors, more than oxygen and pH microelectrodes, require an investment of a significant amount of training time and effort before they can be applied successfully.

4. Applications of Major Significance to Chemical Oceanography

For the remainder of this review microelectrode applications that have had major impacts on the field of chemical oceanography are described. As in any synthesis, this assembly of accomplishments could not include every study, and emphasis is colored by the author's field of expertise. However, it is hoped that the diversity of problems addressable with microelectrodes will become evident and that this summary will illustrate how a basic analytical approach can catch on and advance a scientific discipline.

4.1. Parametrization of Benthic Carbon Fluxes: Organic Matter Oxidation and $CaCO_3$ Dissolution

As a tool applied by chemical oceanographers, microelectrodes have had their greatest impact on studies of benthic carbon cycling. Prior to 1980 there was little information on how much organic carbon reaches the sea floor, what portion is recycled by different diagenetic processes, or how and where organic carbon oxidation impacts $CaCO_3$ dissolution and accumulation. In fact, dissolved oxygen profiles in sediments were rarely measured but instead were often inferred on the basis of coarsely measured distributions of other chemical species such as NO_3^- or Mn^{2+}.[43,44] Oxygen microelectrodes made it possible to assay dissolved oxygen in marine sediments and estimate rates of oxygen production and consumption.[45,46] Oxygen microelectrodes applied together with pH (and in a few cases pCO_2) microelectrodes in situ have provided critical data for constraining rates of calcite dissolution driven by metabolically produced CO_2.[47−49] At this juncture, the importance of the advent of techniques to deploy microelectrodes underwater utilizing landers, submersibles, and remote operated vehicles[6] deserves special mention. Decompression, warming, and sampling disturbance bias rate estimates derived from shipboard measurements. These artifacts have been born out by comparisons of O_2 and pH profiles measured at the sediment−water interface in situ and in recovered cores, and they are especially great for surficial sediments from deep and fauna-rich environments.[46,50,51] Thus, in situ techniques were a prerequisite for the contributions microelectrodes have made to documenting benthic carbon fluxes.

To appreciate carbon fluxes based on in situ microelectrode measurements further, it is essential to understand that organic carbon is the ocean's ultimate reductant that balances changes in dissolved oxygen through the opposing processes of photosynthesis and respiration. Chemical oceanographers can derive benthic organic carbon fluxes from benthic oxygen fluxes provided accounting is also made for burial fluxes of

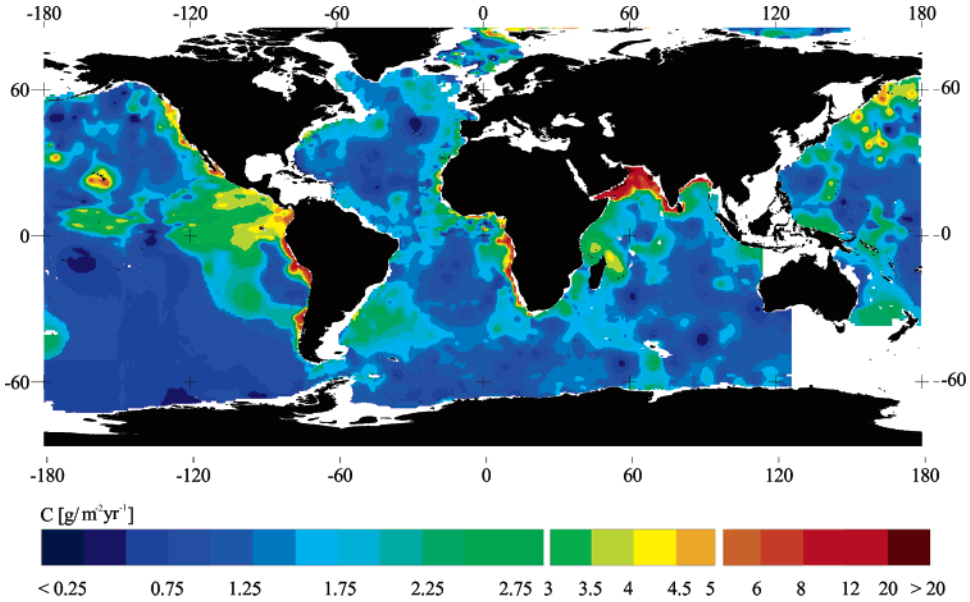

Figure 5. Global distribution pattern of the minimum flux of particulate organic carbon to the sea floor (1° × 1°, >1000 m water depth) based on diffusive oxygen uptake rates derived from in situ oxygen microelectrode measurements across the sediment−water interface. Reproduced with permission from the American Geophysical Union, ref 63. Copyright 2005 American Geophysical Union.

organic carbon and other chemically reduced materials such as pyrite.[52] The latter must be generated as a consequence of anaerobic pathways of organic carbon mineralization and not subsequently oxidized by reactions that contribute to the oxygen uptake.[53] To illustrate the derivation of a benthic carbon oxidation rate, the profiles displayed in Figure 4 indicate a diffusive oxygen utilization rate (DOU) equal to between 0.34 and 0.45 μmol cm^{-2} day^{-1} which equates to a carbon oxidation rate of 11−15 g m^{-2} year^{-1} assuming a molar organic C:O_2 remineralization ratio of 106/138.[54] The primary oxygen utilization rate was derived by applying two similar interpretive methods to the two profiles that originated from the Oregon shelf. The first method sets DOU = D_o (d$C(z)$/dz), where D_o is the temperature-dependent molecular diffusion coefficient of dissolved O_2 and d$C(z)$/dz is the oxygen concentration gradient within the diffusive boundary layer (DBL), an estimated portion of each microprofile extending above the sediment−water interface.[55] In studies designed to specifically map the thickness of the DBL or its dynamics, finer resolution vertical microprofiles are often recorded,[56] and further discussion of the significance of microelectrode measurements of the DBL is presented below. The second method for deriving O_2 consumption rates is based on fitting one or more parabolas to each entire oxygen microprofile as an analytical means to calculate volume-specific O_2 consumption rates (R) that are then integrated over the depth of oxygen penetration. Similarly, individual profiles can be analyzed with a numerical procedure.[57] These computations stem from the one-dimensional mass conservation diagenetic equation under steady-state conditions that for the analytical solution simplifies to $R = \varphi D_s(d^2C/dz^2)$, where φ is the sediment porosity and D_s is the molecular diffusion coefficient for oxygen corrected for the sediment's tortuosity. This formulation assumes zero-order kinetics (i.e., R is not a function of C) and ignores changes in D_s and φ with depth.[57,58] Ideally, both methods should yield the exact same DOU estimate, which was true for profile B but not A in Figure 4 (see caption). Other studies have reported similar comparisons and assessed that the differences were not significant.[50]

An increasing number of investigations of benthic oxygen consumption have paired in situ oxygen microprofiling with benthic chamber determinations of total oxygen uptake (TOU). The resulting flux comparisons have shown that there is enhanced oxygen uptake caused by animal activity (e.g., irrigation) in nearshore marine environments but that DOU ≈ TOU in the deep, pelagic regions of the sea.[59,60] It also has been suggested that there is a correlation, after an initial threshold is exceeded, between total oxygen uptake and nondiffusional pore water transport.[61] The idea behind this relationship is that total oxygen uptake reflects total respiration and therefore increases with benthic infaunal activity. As respiration increases, more biological energy is expended—some of which will be used for irrigation—and nondiffusive transport increases. Meile and Van Cappellen[62] derived generalized relationships of these parameters based on published rates for use in global models. A more recent study presents a global distribution pattern of the minimum flux of particulate organic carbon to the sea floor (water depth >1000 m) based on regionally specific correlations between DOU estimates from 125 locations, the total carbon content in the corresponding surface sediments, and the oxygen concentration in bottom waters.[63] Reproduced in Figure 5, this pattern was then used with a consideration of TOU:DOU ratios on continental margins (water depth < 1000 m) to predict that the total organic carbon flux to the entire ocean floor equals ~0.6 GtC year^{-1} (50 × 10^{12} mol year^{-1}).[50]

Benthic inorganic carbon fluxes on a global scale have also been constrained in part because of in situ microelectrode studies.[64] Because calcium carbonate dissolution in ocean sediments responds to undersaturation in pore waters driven by respiration-produced CO_2, the fine scale distribution of oxygen-consuming processes dictating organic carbon remineralization has been found to be critical to the magnitude of derived rates of calcite dissolution in calcite-rich sediments in the pelagic ocean.[65]

Most representations of calcite dissolution in marine sediments are formulated as a function of the saturation state of the surrounding water with respect to calcite, Ω_c, defined by $\Omega_c = [Ca^{2+}][CO_3^{2-}]/K_{sp,c}$, where $K_{sp,c}$ is the thermody-

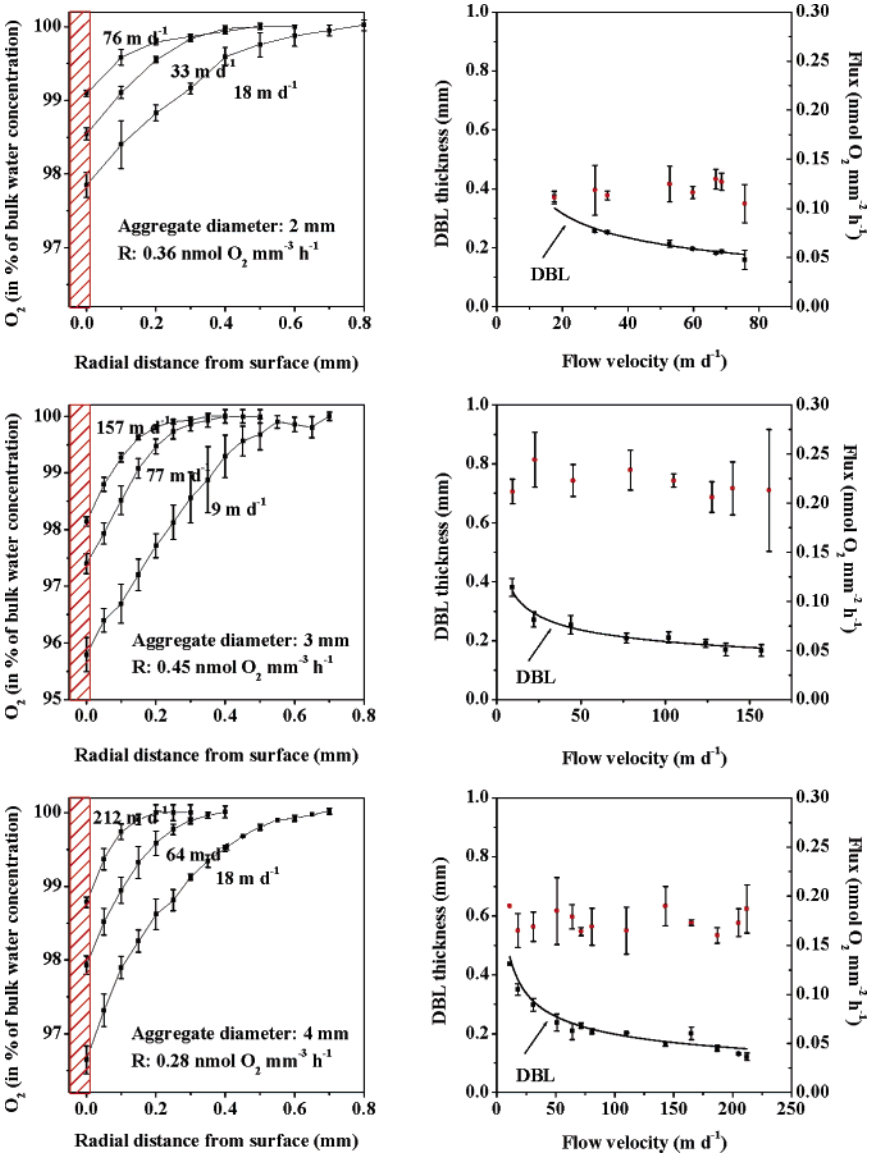

Figure 6. Radial oxygen distributions along the equators of three different marine aggregates at different sinking velocities simulated by flow past the aggregate (left), and the DBL thickness and oxygen fluxes as a function of sinking velocity in the same aggregates (right). Each measuring point represents a mean value, with the SD of the mean value shown as bars ($n = 3$). Reprinted with permission from ref 84. Copyright 2001 American Society of Limnology and Oceanography, Inc.

namic solubility product for calcite at in situ conditions. The rate of calcite dissolution, $R_{d,c}$, is given by an empirical expression $R_{d,c} = k_{d,c}[CaCO_{3(s)}](1 - \Omega_c)^n$, where $k_{d,c}$ represents a rate constant and n the reaction order. Hales and Emerson[66] demonstrated that when oxygen microprofiles are modeled with a two-part exponential dependence on sediment depth, pH microelectrode data are more consistent with a first-order dependence on undersaturation in sediments accumulating near the ocean's saturation horizon. Their analysis also indicates that co-dependent dissolution rate constants only vary by about an order of magnitude. Although not universally accepted, the significance of these microelectrode-based findings is profound. First, they replace long-standing laboratory results that favor an unusual reaction order, $n_c = 4.5$, and rate constants for calcite dissolution up to 6 orders of magnitude greater than those derived from sea-floor observations.[67] Second, the dissolution rates predicted for a number of contrasting pelagic locations become relatively low and consistent with in situ benthic chamber incubations.[65] Thus, although only a relatively few in situ pH microelectrode measurements have been made on the deep sea floor, they have given the chemical oceanographic community an improved understanding of the kinetics of calcium carbon dissolution in pelagic environments. This knowledge has and should continue to be applied with global distributions of respiration rates (such as those leading to Figure 5), water column saturation states, and sediment calcite distributions to predict the dynamics of fossil fuel CO_2 neutralization by marine carbonates.[68]

4.2. Diffusive Boundary Layers and Marine Aggregates

The primary attribute of microelectrodes underlying the scientific highlights given in the previous section is their resolution of chemical changes over small spatial scales without significant disturbance. As reviewed by Boudreau[69] and Jørgensen,[70] a special property of the small scale at the boundary between a flowing fluid and a semisolid surface, such as the sediment−water interface or a macroscopic marine particle, is the dominance of viscous over inertial forces. As the surface is approached within the viscous

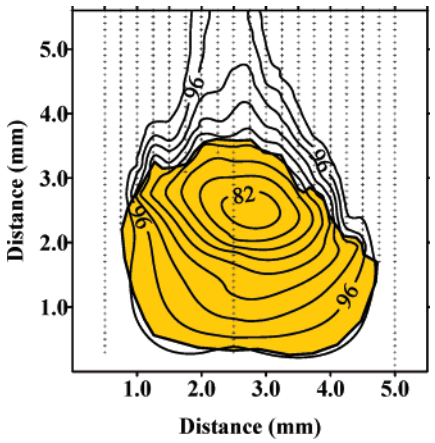

Figure 7. Isopleths of oxygen distribution (in percentage of air saturation) within and around a ~3.5-mm-diameter aggregate in an upward-directed uniform flow field with a velocity of 64 m day^{-1}. The crosses represent the measuring points, and the periphery of shaded area is the boundary of the aggregate mapped by the oxygen sensor under a dissection microscope. Reprinted with permission from ref 84. Copyright 2001 American Society of Limnology and Oceanography, Inc.

sublayer, mass transport becomes dominated by molecular diffusion. This latter thin-film region is called the diffusive boundary layer (DBL), and chemical oceanographers have long recognized that the transfer of solutes through a DBL may impose limits on a number of important chemical processes including organic matter degradation,[71] $CaCO_3$ dissolution,[72] benthic contaminant release,[73] and precipitation of ferromanganese nodules.[74]

Microelectrodes demonstrated the existence and scale of DBLs by revealing persistent oxygen and pH gradients above the sediment−water interface[75] and around flocculent marine snow particles and fecal pellets.[76] Although some compression of the DBL was latter documented as a microelectrode artifact,[77] these gradients were found to be especially pronounced where marine microorganisms, such as those forming microbial mats or bacterial colonies, were highly active, and they signified that processes requiring low oxygen, including denitrification and N_2 fixation, could occur in microenvironments within aerobic marine water columns.[76−79]

A series of later microelectrode studies of the DBL emphasized that chemical gradients in the DBL were actually dynamic features and relationships between water flow velocities, surface roughness, DBL thickness, and biogeochemical rates and pathways were examined.[80−83] As an illustration of this type of innovative study, Figure 6 displays high-resolution radial oxygen distributions and remineralization rates in isolated marine aggregates (diameters 2−3.5 mm) during different flow-simulated sinking velocities as determined by Ploug.[84] Oxygen distributions were shown to be asymmetrical, with a dynamic downstream wake of O_2-undersaturated water (Figure 7). Oxygen concentration differences (from the ambient concentration outside to inside) were a function of the aggregate size and the flow-dependent DBL thickness measured at the aggregate's equator. Under high ambient oxygen concentrations, anoxic conditions could not be produced and organic matter remineralization (as assessed from the nearly constant oxygen fluxes) was reaction limited rather than transport limited. In contrast, once aggregates were no longer sinking (e.g., by sedimentation), exchange rates of solutes between aggregates and the surrounding water were estimated as being significantly

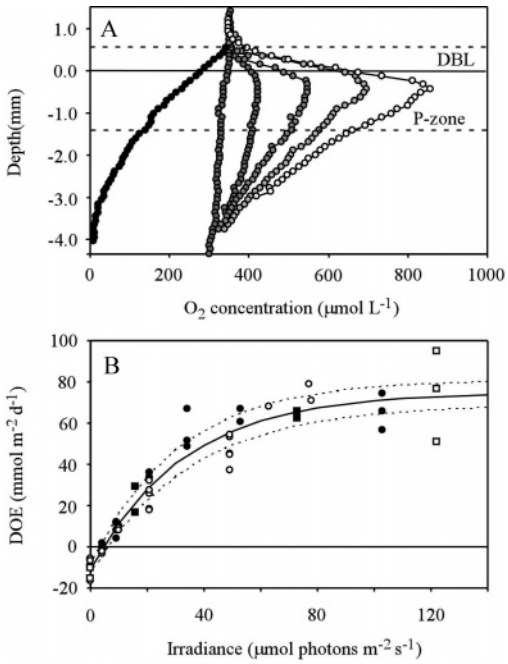

Figure 8. Six O_2 microprofiles measured in diatom-covered sediment recovered from a 20-m station from a high Arctic fjord. To illustrate dynamic changes in O_2 production, measurements were performed at different spots under increasing incident irradiance (0, 4, 9, 21, 53, 103 μmol photons m^{-2} s^{-1}). The horizontal line indicates the position of the sediment surface, while broken lines represent the diffusive boundary layer (DBL) and the photic zone (P-Zone), respectively. (B) As part of the same study, diffusive O_2 exchange was determined as a function of the incident irradiance. Different symbols represent different stations, the solid line represents a fitted function, while dotted lines represent the 95% confidence interval. Reproduced from ref 85 with permission from Inter-Research Journals. Copyright 2002 Inter-Research Journals.

lower because of mass transport limitations. These results illustrate the complexity of processes driving microbial degradation in the ocean during particulate aggregation−disaggregation, transport, and sedimentation. They also provide insight into why differences arise in particle-associated microbial communities and respiration rates between coastal, pelagic, and benthic environments.

4.3. Dynamic Sensing of Photosynthesis and Respiration

Although not stated explicitly, use of DBL gradients to compute diffusive oxygen fluxes between the water column and a macroscopic particle or the water column and sediments is an approach for estimating net oxygen exchange. When particles or sediments are from euphotic waters, the primary production of surface films of microalgae under light conditions can generate oxygen that reverses the sign of the O_2 gradient across the DBL. This dynamic has been demonstrated in many studies, with an example given in Figure 8.[85]

The gross photosynthesis rate during illumination is light intensity, time, and space dependent and can also be resolved with microelectrodes. This technique is applied at different depths (usually 100 or 200 μm intervals) and based on determining the rate of decrease in O_2 concentration over the first 1−2 s after switching from a steady-state light condition to total darkness.[86,87] The critical attributes of the applied oxygen microelectrodes are fast response times and good signal sensitivity (Table 1) in addition to their small

size. Simultaneous microelectrode determinations of net and gross photosynthesis have been used to indicate the percentage of gross photosynthesis consumed within a sediments photic zone. The range for various intertidal phototrophic communities under intermediate light intensities is ~50−80%.[85,88] This can be higher than net O_2 uptake in the dark due to leakage of labile material from photosynthesizing microorganisms and the enhanced oxidation of end products of anaerobic respiration.[89] The heterogeneity and importance of benthic microphyte photosynthesis for total primary production in coastal settings such as a high Arctic fjord[85] have also been extrapolated from such studies. The only other method that has provided roughly comparable benthic photosynthesis estimates are paired light and dark benthic chamber measurements of O_2 and/or CO_2 fluxes.[90]

Other examples of oceanographic investigations that are based on sensor dynamics are studies of water column microstructure[91] and assessments of benthic O_2 uptake rates by interrupted flow[92] or eddy correlation techniques.[93,94] The latter two are considered by many as the most reliable means to assess benthic respiration rates in cases of highly permeable sediments such as sands. By the eddy correlation method, a Clark-type oxygen microelectrode is used with an acoustic Doppler velocimeter to sense (usually at 25 Hz) O_2 concentration and vertical velocity at the same point above the sediment−water interface. This allows computation of the benthic oxygen flux from a time average of the product of the turbulent fluctuations in these parameters.[93] This technique is noninvasive and averages oxygen consumption occurring over a broad sea floor area, the size of which depends on the average flow velocity and sensor height above bottom. In retrospect, it is interesting that the same microelectrode can acquire information about oxygen consumption and production processes for various sediments at both micro- and macroscales.

4.4. Redox Processes, Speciation, and Kinetics

In this section, voltammetric electrodes are highlighted as tools for studying primary and secondary redox reactions and speciation in a host of marine milieus with minimal sampling artifacts. These applications were virtually unheard of before 1995 but are becoming commonplace today. The unique advantage of the either the Ir- or Au-based designs of voltammetric microelectrode is that these sensors can simultaneously detect multiple redox species within a single potential scan. Alternatively, multiple voltammetric methods (e.g., linear sweep, square wave, and/or square-wave anodic or cathodic stripping voltammetry)[10] can be applied in succession to optimize quantitative assessments of diverse chemical species and study species interactions in time series.

To illustrate the detection of short-lived intermediate reaction species and redox species interactions, Figure 9 is taken from a synthesis paper[42] that addresses sulfur speciation in contrasting marine environments. Using cyclic voltammetric scans measured at 1000 mV s^{-1} in situ at a water depth of 2500 m, Luther et al.[42] followed the rapid formation of polysulfides during H_2S oxidation near the tubeworm *Riftia pachyptila* growing in diffusely flowing hydrothermal vent fluids (semi-enclosed by the voltammetric sensor package). They also reported similar S_x^{2-} signals measured in subsurface layers of a saltmarsh microbial mat and in the pore waters of subtidal sediments. From these data and supporting information they deduced that Fe(III) was the direct oxidant in each environment. Coincident and subsequent studies of soluble organic-Fe(III) complexes in laboratory solutions and anoxic sediments[95−98] have confirmed that reactions of soluble Fe(III) with H_2S do form polysulfides and another initially soluble, electroactive, reaction intermediate, FeS.

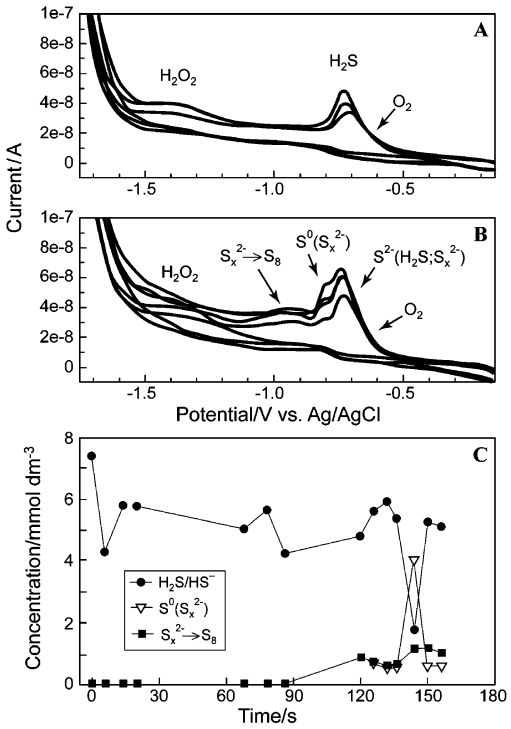

Figure 9. Representative cyclic voltammetry scans measured with a Au-amalgam electrode protected with a counter and reference electrode within a "wand". The wand was positioned with the submersible *Alvin* in diffuse flow near vent tubeworms *R. pachyptila*. (A) Initial 1000 mV s^{-1} scans showing that only O_2 and H_2S coexisted; (B) subsequent 1000 mV s^{-1} scans showing that polysulfides formed from S^0 and S^{-2}; (C) time course showing the rapid change in sulfur speciation at this tubeworm location. Redrawn from ref 42 with permission from The Royal Society of Chemistry. Copyright 2001 The Royal Society of Chemistry.

Why is this work extraordinary? Because by maintaining a Au/Hg microelectrode in a harsh, natural environment there was a certainty that biogeochemical processes were being followed (e.g., in the rapid time course displayed in Figure 9) instead of artifacts of sample manipulation. In addition, in the ensuing sediment work it was shown that formation of soluble FeS from organic Fe(III) complexes and sulfide can enhance pyrite precipitation[98] and precipitation cycles in nearshore sediments can be seasonal.[99] These findings help explain the environmental factors that promote immobilization of Fe and S as reduced sedimentary minerals. Global Fe and S cycles have varied over geologic time because of this sink.

A second example of the utility of voltammetric microelectrodes again illustrates how the progress of redox reactions can be followed in real time within biologically active systems without sampling artifacts. In studies of the anaerobic respiration of marine bacteria, controlled introduction of electron acceptors to batch cultures is an established method for determining what kinetic factors may cause redox reaction sequences to deviate from purely thermodynamic predictions. These factors include the available enzyme systems of different bacterial strains, the chemical form of the electron acceptor, and, for insoluble substrates, surface limitations imposed by the ratio of concentration to bacterial cell density.

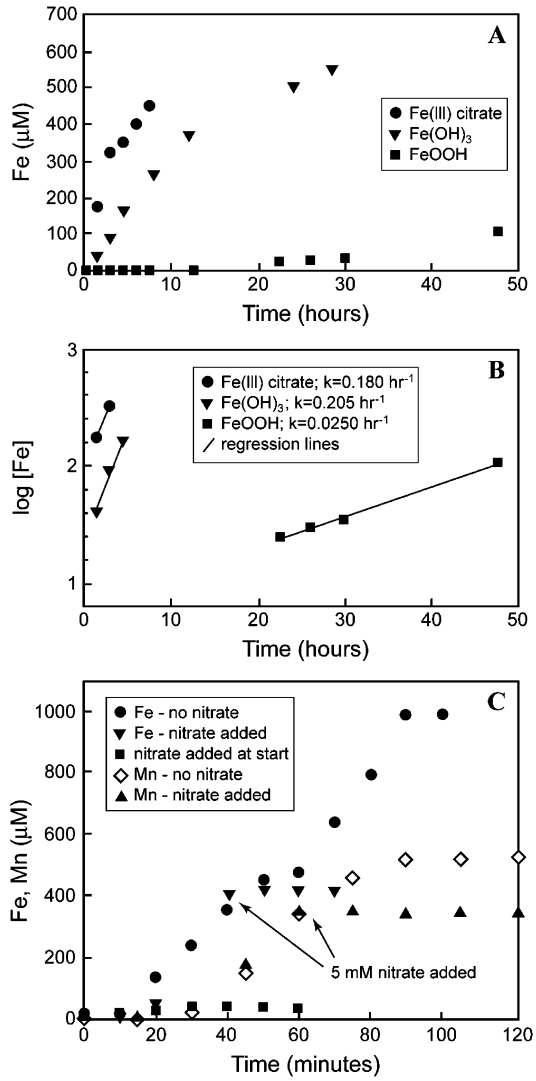

Figure 10. (A) Time-course voltammetric microelectrode data of the reduction of 500 μM quantities of three Fe(III) phases by *S. putrefuaciens* strain MR-4; (B) semilog plot of the time course data used to determine pseudo-first-order rate constants; (C) competition experiments in which nitrate was added to cultures already growing on Fe(III) citrate or amorphous MnO_2. Redrawn from ref 100 with permission from Elsevier. Copyright 2000 Elsevier.

Dollhopf et al.[100] followed the reduction of Mn and Fe by direct voltammetric measurement[101] in cultures of *Shewanella putrefaciens*, a facultative anaerobic bacterium isolated from the suboxic zone of the Black Sea. One selection of data (Figure 10A and B) shows the derivation of pseudo-first-order rate constants for the respiration of three different forms of Fe(III). A second data selection (Figure 10C) displays the results of experiments in which nitrate was introduced to compete with amorphous MnO_2 and Fe(III) citrate. Both datasets indicate that marine bacteria will utilize a soluble chemical oxidant before a colloidal mineral. A significant time lag before reduction was also only observed with insoluble electron acceptors, implying cells must first orient to mineral surfaces.

The chemical oceanographic relevance of these experiments can only be briefly explored here. Certainly the kinetic information is important for comparing biotic and abiotic reaction rates in the natural environment. Furthermore, the competition experiment suggests a microbiological reason for a slower onset of metal oxide reduction in suboxic environments replete in nitrate. This biological control is not equivalent to the suggestion that microbial nitrate reduction (denitrification) competes with the chemical reduction of nitrate with Mn(II) (because the latter implies concurrent MnO_2 reduction). Field evidence that sparked debate about Mn and N interactions began with voltammetric Au/Hg electrode profiles in continental margin sediments documenting separation between where O_2 is depleted and the appearance of Mn(II).[102]

In the future it is anticipated that gel-integrated Hg-plated Ir-based microelectrodes may be used in studies similar to those just cited in order to follow rapid reaction-based changes in trace metal speciation. To date, the primary emphases of groups employing these sensors have been comparing dynamic (i.e., mobile through the gel) trace metal concentrations (particularly for the metals Pb, Cd, Zn, Mn, and Cu) to total (ICP−MS measured) concentrations in lakes and estuaries and establishing the dependence of speciation on other environmental factors such as pH, salinity, turbidity, and water depth.[10,37] In such studies there is greater complexity when interpreting long time-series data because the effects of both water mass transport and biogeochemical reactions are being sensed. However, there is also the capability of building detailed spatial and temporal data banks for ecosystems through which the sources, sinks, and exchanges of different trace metal forms can be thoroughly described.[10]

5. Concluding Remarks

Microelectrodes are analytical tools, but there is also considerable engineering, art, and science behind their application. The microelectrodes that have been applied widely in the ocean are still very few. This review has stressed the breadth of microelectrode-based information that has been gained about ocean chemistry since Revsbech et al.[103] first reported using microelectrodes to measure O_2 profiles in coastal sediments. No one could have predicted at that time the inventiveness of these applications. Their variety has constrained fundamental biogeochemical processes at many temporal and spatial scales under a host of environmental and laboratory conditions. The examples in this review should inspire ongoing development efforts to produce additional reliable and durable microsensors for field applications. Certainly, the recent and rapid extension of fiber and planar optodes to sediment and water column studies has grown out of microelectrode approaches.[104−106] Further development and experimentation needs only the objective to generate high-quality sensor data for environmentally sensitive marine chemical species. Students also need to be trained in the fundamentals of electrochemistry in order to fully understand the subtleties of an electrode response. With better sensors and more trained marine analysts, the science discoveries will come and new data will form the basis of global biogeochemical models. This is especially certain as marine scientists enter into initiatives for widespread ocean observing as is planned for the next decade.[107]

6. Acknowledgments

C.E.R. gratefully acknowledges support from the Office of Naval Research under Award No. N000140610212.

7. References

(1) Buffle, J.; Horvai, G. In *In Situ Monitoring of Aquatic Systems: Chemical Analysis and Speciation*; Buffle, J., Horvai, G., Eds.;

IUPAC Series on Analytical and Physical Chemistry of Environmental Systems; Wiley: Chichester, 2000; Vol. 6, pp 1−18.
(2) Taillefert, M.; Luther, G. W., III; Nuzzio, D. B. *Electroanalysis* **2000**, *12*, 401.
(3) Buffle, J.; Tercier-Waeber, M.-L. In *In Situ Monitoring of Aquatic Systems: Chemical Analysis and Speciation*; Buffle, J., Horvai, G., Eds.; IUPAC Series on Analytical and Physical Chemistry of Environmental Systems; Wiley: Chichester, 2000; Vol. 6, pp 279−406.
(4) Štulík, K.; Amatore, C.; Holub, K.; Mareček, V.; Kutner, W. *Pure Appl. Chem.* **2000**, *72*, 1483.
(5) Revsbech, N. P.; Jørgensen, B. B. In *Advances in Microbial Ecology*; Marshall, K. C., Ed.; Plenum: New York, 1986; Vol. 9, pp 293−352.
(6) Reimers, C. E.; Glud, R. N. In *Chemical Sensors in Oceanography*; Varney, M., Ed.; Gordon and Breach: Amsterdam, 2000; pp 249−282.
(7) Kühl, M.; Revsbech, N. P. In *The Benthic Boundary Layer: Transport Processes and Biogeochemistry*; Boudreau, B. P., Jørgensen, B. B., Eds.; Oxford University Press: New York, 2001; pp 180−203.
(8) de Beer, D. In *In Situ Monitoring of Aquatic Systems: Chemical Analysis and Speciation*; Buffle, J., Horvai, G., Eds.; IUPAC Series on Analytical and Physical Chemistry of Environmental Systems; Wiley: Chichester, 2000; Vol. 6, pp 161−194.
(9) Revsbech, N. P.; Kjaer, T.; Damgaard, L. R.; Lorenzen, J.; Larsen, L. H. In *In Situ Monitoring of Aquatic Systems: Chemical Analysis and Speciation*; Buffle, J., Horvai, G., Eds.; IUPAC Series on Analytical and Physical Chemistry of Environmental Systems; Wiley: Chichester, 2000; Vol. 6, pp 195−222.
(10) Buffle, J.; Tercier-Waeber, M.-L. *Trends Anal. Chem.* **2005**, *24*, 172.
(11) Revsbech, N. P. *Limnol. Oceanogr.* **1989**, *34*, 472.
(12) Revsbech, N. P. In *Polarographic Oxygen Sensors: Aquatic and Physiological Applications*; Gnaiger, E., Forstner, H., Eds.; Springer: Heidelberg, 1983; pp 265−273.
(13) Reimers, C. E. *Deep-Sea Res.* **1987**, *34*, 2019.
(14) Gundersen, J. K.; Ramsing, N. B.; Glud, R. N. *Limnol. Oceanogr.* **1998**, *43*, 1932.
(15) Fatt, I. *Polarographic Oxygen Sensors*; CRC Press: Cleveland, 1976; 278 pp.
(16) Hitchman, M. L. *Measurement of Dissolved Oxygen*; Wiley and Sons: New York, 1978; 255 pp.
(17) Cottrell, F. G. *Z. Phys. Chem.* **1902**, *42*, 385.
(18) Brett, C. M. A.; Brett, A. M. O. *Electrochemistry Principles, Methods, and Applications*; Oxford University Press: Oxford, 2002; 427 pp.
(19) Glud, R. N.; Gundersen, J. K.; Ramsing, N. B. In *In Situ Monitoring of Aquatic Systems: Chemical Analysis and Speciation*; Buffle, J., Horvai, G., Eds.; IUPAC Series on Analytical and Physical Chemistry of Environmental Systems; Wiley: Chichester, 2000; Vol. 6, pp 19−73.
(20) Bates, R. G. *Determination of pH, Theory and Practice*; Wiley: New York, 1973; 479 pp.
(21) Thomas, R. C. In *Intracellular pH*: *Its Measurement, Regulation, and Utilization in Cellular Functions*; Alan R. Liss: New York, 1982; pp 1−6.
(22) Zhao, P.; Cai, W.-J. *Anal. Chim. Acta* **1999**, *395*, 285.
(23) Li, C.-Y.; Zhang, X.-B.; Han, Z.-X.; Åkermark, B.; Sun, L.; Shen, G.-L.; Yu, R.-Q. *Analyst* **2006**, *131*, 388.
(24) Wang, Y; Yuan, H.; Lu, X.; Zhou, Z.; Xiao, D. *Electroanalysis* **2006**, *18*, 1493.
(25) Cai, W.-J.; Reimers, C. E. In *In Situ Monitoring of Aquatic Systems: Chemical Analysis and Speciation*; Buffle, J., Horvai, G., Eds.; IUPAC Series on Analytical and Physical Chemistry of Environmental Systems; Wiley: Chichester, 2000; Vol. 6, pp 75−120.
(26) Cai, W.-J.; Reimers, C. E. *Limnol. Oceanogr.* **1993**, *38*, 1776.
(27) Komada, T.; Reimers, C. E.; Boehme, S. E. *Limnol. Oceanogr.* **1998**, *43*, 769.
(28) Thomas, R. C. *Ion-Sensitive Intracellular Microelectrodes, How to Make and Use Them*; Academic Press: London and New York, 1978.
(29) de Jong, S. A.; Hofman, P. A. G.; Sandee, A. J. J. *Mar. Ecol. Prog. Ser.* **1988**, *45*, 187.
(30) Tercier, M. L.; Parthasarathy, N.; Buffle, J. *Electroanalysis* **1995**, *7*, 55.
(31) Brendel, P. J.; Luther, G. W., III. *Environ. Sci. Technol.* **1995**, *29*, 751.
(32) Tercier, M.-L.; Buffle, J. *Anal. Chem.* **1996**, *68*, 3670.
(33) Luther, G. W., III; Reimers, C. E.; Nuzzio, D. B.; Lovalvo, D. *Environ. Sci. Technol.* **1999**, *33*, 4352.
(34) For measurements of Pb and Cd with subnanomolar detection, SWASV conditions: deposition potential = −1.200V; deposition time = 15 min; scan potentials from −1.2 to −0.1 V; pulse amplitude = 25 mV; step amplitude = 8 mV; frequency = 50 Hz (ref 30).
(35) Belmont, C.; Tercier, M.-L.; Buffle, J.; Fiabccabrino, G. C.; Koudelka-Hep, M. *Anal. Chim. Acta* **1996**, 203.
(36) Tercier-Waeber, M.-L.; Pei, J.; Buffle, J.; Fiaccabrino, G. C.; Koudelka-Hep, M.; Riccardi, G.; Confalonieri, F.; Sina, A.; Graziottin, F. *Electroanalysis* **2000**, *12*, 27.
(37) Tercier-Waeber, M.-L.; Confalonieri, F.; Riccardi, G.; Sina, A.; Nöel, S.; Buffle, J.; Graziottin, F. *Mar. Chem.* **2005**, *97*, 216.
(38) Van Leeuwen, H. P.; Town, R. M.; Buffle, J.; Cleven, R. F. M. J.; Davidson, W.; Puy, J.; Van Riemsdijk, W. H.; Sigg, L. *Environ. Sci. Technol.* **2005**, *39*, 8545.
(39) Luther, G. W., III; Brendel, P. J.; Lewis, B. L.; Sundby, B.; Lefrancois, L.; Silverberg, N.; Nuzzio, D. B. *Limnol. Oceanogr.* **1998**, *43*, 325.
(40) Sundby, B.; Caetano, M.; Vale, C.; Gobeil, C.; Luther, G. W., III; Nuzzio, D. B. *Environ. Sci. Technol.* **2005**, *39*, 2080.
(41) Reimers, C. E.; Stecher, H. A., III; Taghon, G. L.; Fuller, C. M.; Huettel, M.; Rusch, A.; Ryckelynck, N.; Wild, C. *Cont. Shelf Res.* **2004**, *24*, 183.
(42) Luther, G. W., III; Glazer, B. T.; Hohmann, L.; Popp, J. I.; Taillefert, M.; Rozan, T. F.; Brendal, P. J.; Theberge, S. M.; Nuzzio, D. B. *J. Environ. Monit.* **2001**, *3*, 61.
(43) Murray, J. W.; Grundmanis, V. *Nature* **1980**, *209*, 1527.
(44) Goloway, F.; Bender, M. *Limnol. Oceanogr.* **1982**, *27*, 624.
(45) Revsbech, N. P.; Sørensen, J.; Blackburn, T. H.; Lomholt, J. P. *Limnol. Oceanogr.* **1980**, *25*, 403.
(46) Reimers, C. E.; Fischer, K. M.; Merewether, R.; Smith, K. L., Jr.; Jahnke, R. A. *Nature* **1986**, *320*, 741.
(47) Archer, D.; Emerson, S.; Reimers, C. *Geochim. Cosmochim. Acta* **1989**, *53*, 2831.
(48) Cai, W.-J.; Reimers, C. E.; Shaw, T. J. *Geochim. Cosmochim. Acta* **1995**, *59*, 497.
(49) Hales, B.; Emerson, S. *Global Biogeochem. Cycles* **1996**, *10*, 527.
(50) Glud, R. N.; Gundersen, J. K.; Jørgensen, B. B.; Revsbech, N. P.; Schulz, H. D. *Deep-Sea Res.* **1994**, *41*, 1767.
(51) Reimers, C. E.; Ruttenberg, K. C.; Canfield, D. E.; Christiansen, M. B.; Martin, J. B. *Geochim. Cosmochim. Acta* **1996**, *60*, 4037.
(52) Jahnke, R. A. *Global Biogeochem. Cycles* **1996**, *10*, 71.
(53) Canfield, D. E.; Jørgensen, B. B.; Fossing, H.; Glud, R.; Ramsing, N. B.; Thamdrup, B.; Hansen, J. W.; Nielsen, L. P.; Hall, P. O. J. *Mar. Geol.* **1993**, *113*, 27.
(54) Froelich, P. N.; Klinkhammer, G. P.; Bender, M. L.; Luedtke, N. A.; Heath, G. R.; Cullen, D.; Dauphin, P.; Hammond, D.; Hatman, B.; Maynard, V. *Geochim. Cosmochim. Acta* **1979**, 43, 1075.
(55) Gundersen, J. K.; Jørgensen, B. B. *Nature* **1990**, *345*, 604.
(56) Jørgensen, B. B.; Des Marais, D. J. *Limnol. Oceanogr.* **1990**, *35*, 1343.
(57) Berg, P.; Risgaard-Petersen, N.; Rysgaard, S. *Limnol. Oceanogr.* **1998**, *43*, 1500.
(58) Rassmussen, H.; Jørgensen, B. B. *Mar. Ecol. Prog. Ser.* **1992**, *81*, 289.
(59) Archer, D.; Devol, A. *Limnol. Oceanogr.* **1992**, *37*, 614.
(60) Wenzhöfer, F.; Glud, R. N. *Deep-Sea Res.* **2002**, *49*, 1255.
(61) Jahnke, R. In *The Benthic Boundary Layer Transport Processes and Biogeochemistry*; Boudreau, B. P., Jørgensen, B. B., Eds.; Oxford: New York, 2001; pp 302−319.
(62) Meile, C.; Van Cappellen, P. *Limnol. Oceanogr.* **2003**, *48*, 777.
(63) Seiter, K.; Hensen, C.; Zabel, M. *Global Biogeochem. Cycles* **2005**, *19*, GB1010.
(64) Archer, D. *Global Biogeochem. Cycles* **1996**, *10*, 511.
(65) Hales, B. *Paleocean* **2003**, *18*, 1099, doi: 10.1029/2003PA000915.
(66) Hales, B.; Emerson, S. *Earth Plant. Sci. Lett.* **1997**, *148*, 317.
(67) Kier, R. S. *Geochim. Cosmochim. Acta* **1980**, *44*, 241.
(68) Archer, D.; Kheshgi, H.; Maier-Reimer, E. *Global Biogeochem. Cycles* **1998**, *12*, 259.
(69) Boudreau, B. P. In *The Benthic Boundary Layer Transport Processes and Biogeochemistry*; Boudreau, B. P., Jørgensen, B. B., Eds.; Oxford: New York, 2001; pp 104−126.
(70) Jørgensen, B. B. In *The Benthic Boundary Layer Transport Processes and Biogeochemistry*; Boudreau, B. P., Jørgensen, B. B., Eds.; Oxford: New York, 2001; pp 348−373.
(71) Archer, D.; Emerson, S.; Smith, C. R. *Nature* **1989**, *340*, 623.
(72) Boudreau, B. P.; Guinasso, N. L. In *The Dynamic Environment of the Sea Floor*; Fanning, K. A., Manheim, F. T., Eds.; Lexington Books: Lexington 1982; pp 115−145.
(73) Thibodeaux, L. J.; Chang, L.-K.; Lewis, D. J. In *Contaminants and Sediments*; Baker, R. A., Ed.; Ann Arbor Science: Ann Arbor, 1980; Vol. 1pp 349−371.
(74) Santchi, P. H.; Anderson, R. F.; Fleisher, M. Q.; Bowles, W. *J. Geophys. Res.* **1991**, *96*, 10641.
(75) Jørgensen, B. B.; Revsbech, N. P. *Limnol. Oceanogr.* **1985**, *30*, 111.
(76) Alldredge, A. L.; Cohen, Y. *Science* **1987**, *235*, 689.
(77) Glud, R. N.; Gundersen, J. K.; Revsbech, N. P.; Jørgensen, B. B. *Limnol. Oceanogr.* **1994**, *39*, 462.

(78) Paerl, H. W.; Prufert, L. E. *Appl. Environ. Microbiol.* **1987**, *53*, 1078.
(79) Paerl, H. W.; Bebout, B. M. *Science* **1988**, *241*, 442.
(80) Gundersen, J. K.; Jørgensen, B. B. *Nature* **1990**, *345*, 604.
(81) Jørgensen, B. B.; Des Marais, D. J. *Limnol. Oceanogr.* **1990**, *35*, 1343.
(82) Güss, S. *Estuar. Coast. Shelf Sci.* **1998**, *46*, 143.
(83) Røy, H.; Huettel, M.; Jørgensen, B. B. *Limnol. Oceanogr.* **2004**, *49*, 686.
(84) Ploug, H. *Limnol. Oceanogr.* **2001**, *46*, 1624.
(85) Glud. R. N.; Kühl, M.; Wenzhöfer, F.; Rysgaard, S. *Mar. Ecol. Prog. Ser.* **2002**, *238*, 15.
(86) Revsbech, N. P.; Jørgensen, B. B. *Limnol. Oceanogr.* **1983**, *28*, 749.
(87) Glud, R. N.; Ramsing, N. B.; Revsbech, N. P. *Jour. Phycol.* **1992**, *28*, 51.
(88) Epping, E. H. G.; Jørgensen, B. B. *Mar. Ecol. Prog. Ser.* **1996**, *139*, 193.
(89) Fenchel, T.; Glud, R. N. *Ophelia* **2000**, *53*, 159.
(90) Jahnke, R. A.; Nelson, J. R.; Marinelli, R. L.; Eckman, J. E. *Cont. Shelf Res.* **2000**, *20*, 109.
(91) Oldham, C. *Limnol. Oceanogr.* **1994**, *39*, 1959.
(92) Polerecky, L.; Franke, U.; Werner, U.; Grunwald, B.; de Beer, D. *Limnol. Oceanogr. Methods* **2005**, *3*, 75.
(93) Berg, P.; Røy, H.; Janssen, F.; Meyer, V.; Jørgensen, B. B.; Huettel, M.; de Beer, D. *Mar. Ecol. Prog. Ser.* **2003**, *261*, 75.
(94) Kuwae, T.; Kamio, K.; Inoue, T.; Miyoshi, E.; Uchiyama, Y. *Mar. Ecol. Prog. Ser.* **2006**, *307*, 59.
(95) Rozan, T. F.; Theberge, S. M.; Luther, G. W., III. *Anal. Chim. Acta* **2000**, *415*, 175.
(96) Taillefert, M.; Bono, A. B.; Luther, G. W., III. *Environ. Sci. Technol.* **2000**, *34*, 2169.
(97) Taillefert, M.; Hover, V. C.; Rozan, T. F.; Theberge, S. M.; Luther, G. W., III. *Estuaries* **2002**, *25*, 1088.
(98) Carey, E.; Taillefert, M. *Limnol. Oceanogr.* **2005**, *50*, 1129.
(99) Taillefert, M.; Rozan, T. F.; Glazer, B. T.; Herszage, J.; Trouwborst, R. E.; Luther, G. W., III In *Environmental Electrochemistry Analyses of Trace Element Biogeochemistry*; Taillefert, M., Rozen, T. F., Eds.; ACS Symposium Series 811; American Chemical Society, Washington, DC, 2002; pp 247−264.
(100) Dollhopf, M. E.; Nealson, K. H.; Simon, D. W.; Luther, G. W., III *Mar. Chem.* **2000**, *70*, 171.
(101) They used square-wave voltammetry with a conditioning step of 5−10 s at −0.7 V; scan rate = 250 mV s^{-1}; scan range 0 to −2.1 V; pulse height = 24 mV; 1-mV step increment.
(102) Luther, G. W., III; Sundby, B.; Lewis, B. L.; Brendel, P. J.; Silverberg, N. *Geochim. Cosmochim. Acta* **1997**, *61*, 4043.
(103) Revsbech, N. P.; Jørgensen, B. B.; Blackburn, T. H. *Science* **1980**, *207*, 1355.
(104) Holst, G; Klimant, I.; Kühl, M.; Kohls, O. In *Chemical Sensors in Oceanography*; Varney, M. S., Ed.; Gordon and Breach: Amsterdam, 2000; pp 143−188.
(105) Glud, R. N.; Tengberg, A.; Kühl, M.; Hall, P. O. J.; Klimant, I. *Limnol. Oceanogr.* **2001**, *46*, 2073.
(106) Zhu, Q.; Aller, R. C.; Fan, Y. *Environ. Sci. Technol.* **2005**, *39*, 3906.
(107) ORION Executive Steering Committee; Ocean Observatories Initiative Science Plan: Washington, D.C. 2005, 102 pp.

CR050363N